Hydridic Character and Reactivity of Di[1,2-bis-(dimethylphosphino)ethane]hydridonitrosylmolybdenum(0)

Fupei Liang, Helmut W. Schmalle, Thomas Fox, and Heinz Berke*

Anorganisch-chemisches Institut, Universität Zürich, Winterthurerstrasse 190, CH-8057 Zürich, Switzerland

Received December 20, 2002

The synthesis of the tetraphosphine-substituted molybdenum hydride complex *trans*-Mo(dmpe)$_2$(H)(NO) (**3**) (dmpe = bis(dimethylphosphino)ethane) is described, which is obtained by starting from the known compound Mo(CO)$_4$(NO)(ClAlCl$_3$) via the isolable chloride *trans*-Mo(Cl)(dmpe)$_2$(NO) (**1**) and the borohydride *trans*-Mo(η^1-BH$_4$)(dmpe)$_2$(NO) (**2**). Two deuteride complexes *trans*-Mo(dmpe)$_2$(D)(NO) (**3a**) and *mer*-Mo(CO)(D)(NO)(PMe$_3$)$_3$ (**4**) have been prepared. From these the Mo−D bond ionicities of both deuterides were obtained via determinations of the deuterium quadrupole coupling constants (DQCC) in solution from $T_{1\min}$ measurements of the ^{2}H nucleus and in solid state from static ^{2}H NMR spectra. A strongly polar character of the Mo−D(H) bond was found for **3** and **4**. In agreement with its enhanced hydridicity **3** revealed a very high propensity for hydride transfer reactions. It reacted readily with benzophenone, acetophenone, and acetone to afford the corresponding alkoxide complexes *trans*-Mo(dmpe)$_2$(NO)(OCHRR′) (R = R′ = Ph (**5**); R = Me, R′ = Ph (**6**); R = R′ = Me (**7**)). **3** also underwent rapid insertion with Fe(CO)$_5$ and Re$_2$(CO)$_{10}$ to afford μ-formyl complexes Mo(dmpe)$_2$(NO)[(μ-OCH)Fe(CO)$_4$] (**8**) and Mo(dmpe)$_2$(NO)[(μ-OCH)Re$_2$(CO)$_9$] (**9**), respectively. Furthermore, reversible double insertion of **3** into Re$_2$(CO)$_{10}$ was observed, which furnished the (ON)(dmpe)$_2$Mo(μ-OCH)Re$_2$(CO)$_8$(μ-CHO)Mo(dmpe)$_2$(NO) complex (**10**). For this reaction equilibrium constants were determined by VT-NMR measurements. ΔH and ΔS amount to -58.8 ± 2.7 kJ mol^{-1} and -48 ± 2 J·K^{-1}.mol^{-1}. The reaction of **3** with Mn$_2$(CO)$_{10}$ gave the μ-carbonyl complex Mo(dmpe)$_2$(NO)[(μ-OC)Mn(CO)$_4$] (**12**) via the intermediacy of Mo(dmpe)$_2$(NO)[(μ-OCH)Mn$_2$(CO)$_9$] (**11**). The structures of compounds **1**, **2**, **8**, **9**, **10**, and **12** were studied by single-crystal X-ray diffraction.

Introduction

Transition metal hydrides are useful reagents in many stoichiometric reactions and important intermediates in a large number of catalytic conversions.[1] In many such hydrogenations using transition metal hydrides the proper balance of proton or hydride transfer capabilities is important.[2] In particular, this is the case for ionic hydrogenations occurring with formal splitting of H_2 into H^- and H^+ and the formation of transition metal hydrides with a pronounced hydridic character. For many years our group has systematically investigated the ligand sphere tuning of the character of the L_nM-H bond.[3] In this context, a series of octahedral transition metal hydrides with nitrosyl or carbyne groups as trans-ligands and additionally strongly σ-donating phosphines as cis-ligands have been studied.[4] The L_nM-H bond in such compounds was characterized by their dihydrogen bonding capabilities with weakly acidic substrates,[5] bond ionicity determinations,[6] and insertion behavior as a chemical measure for their hydride transfer capabilities.[7] These studies allowed conclusions on the hydridic character of the hydride ligands as the crucial electronic factor for reactivity.

We have previously reported studies on the chemistry of *mer*-Mo(CO)(H)(NO)(PMe$_3$)$_3$.[8] This hydride shows an unusually high propensity to undergo the carbonyl

(1) (a) Parshall, G. W.; Ittel, S. D. *Homogeneous Catalysis*, 2nd ed.; John Wiley & Sons: New York, 1992. (b) Darensbourg, M. Y.; Ash, C. E. *Adv. Organomet. Chem.* **1987**, *27*, 1. (c) Brunet, J. J. *Eur. J. Inorg. Chem.* **2000**, 1377. (d) Bäckvall, J.-E. *J. Organomet. Chem.* **2002**, *652*, 105.

(2) (a) Hembre, R. T.; McQueen, S. *J. Am. Chem. Soc.* **1994**, *116*, 2141. (b) Bullock, R. M.; Voges, M. H. *J. Am. Chem. Soc.* **2000**, *122*, 12594. (c) Magee, M. P.; Norton, J. R. *J. Am. Chem. Soc.* **2001**, *123*, 1778. (d) Casey, C. P.; Singer, S. W.; Powell, D. R.; Hayashi, R. K.; Kavana, M. *J. Am. Chem. Soc.* **2001**, *123*, 1090. (e) Voges, M. H.; Bullock, R. M. *J. Chem. Soc., Dalton Trans.* **2002**, 759.

(3) (a) Berke, H.; Burger, P. *Comments Inorg. Chem.* **1994**, *16*, 279. (b) Jacobsen, H.; Berke, H. In *Recent Advances in Hydride Chemistry*; Poli, R., Peruzzini, M., Eds.; Elsevier: Amsterdam, 2001; p 89. Kubas, G. J. *Metal Dihydrogen and σ-Bond Complexes, Structures, Theory and Reactivity*; Kluwer Academic/Plenum Press: New York, 2001.

(4) (a) van der Zeijden, A. A. H.; Sontag, C.; Bosch, H. W.; Shklover, V.; Berke, H.; Nanz, D.; von Philipsborn, W. *Helv. Chim. Acta* **1991**, *74*, 1194. (b) Jänicke, M.; Hund, H.-U.; Berke, H. *Chem. Ber.* **1991**, *124*, 719. (c) van der Zeijden, A. A. H.; Bürgi, T.; Berke, H. *Inorg. Chim. Acta* **1992**, *201*, 131. (d) Gusev, D. G.; Nietlispach, D.; Vimenits, A.; Bakhmutov, V. I.; Berke, H. *Inorg. Chem.* **1993**, *32*, 3270. (e) Bakhmutov, V. I.; Bürgi, T.; Burger, P.; Ruppli, U.; Berke, H. *Organometallics* **1994**, *13*, 4203. (f) Gusev, D. G.; Llamazares, A.; Artus, G.; Jacobsen, H.; Berke, H. *Organometallics* **1999**, *18*, 75. (g) Baur, J.; Jacobsen, H.; Burger, P.; Artus, G.; Berke, H.; Dahlenburg, L. *Eur. J. Inorg. Chem.* **2000**, 1423. (h) Bannwart, E.; Jacobsen, H.; Furno, F.; Berke, H. *Organometallics* **2000**, *19*, 3605.

(5) (a) Shubina, E. S.; Belkova, N. V.; Krylov, A. N.; Vorontsov, E. V.; Epstein, L. M.; Gusev, D. G.; Niedermann, M.; Berke, H. *J. Am. Chem. Soc.* **1996**, *118*, 1105. (b) Belkova, N. V.; Shubina, E. S.; Ionidis, A. V.; Epstein, L. M.; Jacobsen, H.; Messmer, A.; Berke, H. *Inorg. Chem.* **1997**, *36*, 1522. (c) Messmer, A.; Jacobsen, H.; Berke, H. *Chem. Eur. J.* **1999**, *5*, 3341.

(6) Nietlispach, D.; Bakhmutov, V. I.; Berke, H. *J. Am. Chem. Soc.* **1993**, *115*, 9191.

10.1021/om021032t CCC: $25.00
Publication on Web 07/16/2003

insertion, which was mainly attributed to the trans influence of the NO ligand and the three trimethylphosphine moieties. On this basis we decided to study a hydride, with four cis phosphorus donors in the coordination sphere of the molybdenum center. For synthetic reasons *trans*-Mo(dmpe)$_2$(H)(NO) bearing two 1,2-bis(dimethylphosphino)ethane (dmpe) ligands with four phosphorus donor links seemed to be an appropriate choice. We anticipated that *trans*-Mo(dmpe)$_2$(H)(NO) would show optimum tuning properties and that it therefore would exhibit a highly activated Mo−H bond. It was indeed found that this complex inserted not only molecules with C═O double bonds, like ketones and metal carbonyl compounds, but also imine compounds with the normally quite reluctant C═N double bond. In this paper, we will present the synthesis, the Mo−H bond ionicity determination, and the carbonyl insertion behavior of *trans*-Mo(dmpe)$_2$(H)(NO). The insertion reaction of Mo(dmpe)$_2$(H)(NO) with imines to afford amido complexes will be reported elsewhere.

Results and Discussions

Synthesis and Characterization of *trans*-Mo(dmpe)$_2$(H)(NO) (3). To our knowledge the only previously reported molybdenum hydride with nitrosyl and bidentate phosphine ligands is *trans*-[MoH(NO)(dppe)$_2$].[9] It was prepared refluxing a mixture of *trans*-[Mo(N$_2$)$_2$(dppe)$_2$], diethyl-*N*-nitrosoamine, and methanol in THF under irradition, or by heating *trans*-[Mo(OH)(NO)(dppe)$_2$] in methanol. However, these procedures seemed to be very special and not suitable for generalization, because, as we will see later for the hydride with dmpe ligands, methanol may react with such highly hydridic hydride. As previously reported[8] the hydride *mer*-Mo(CO)(H)(NO)(PMe$_3$)$_3$ was readily accessible starting from the known compound *trans*-Mo(CO)$_4$(NO)(ClAlCl$_3$) via the corresponding chloride and borohydride intermediates. We considered that access to the hydride with dmpe ligands may also be achieved by a related route. Indeed, the hydride *trans*-Mo(dmpe)$_2$H(NO) (**3**) can be obtained via the isolable compounds Mo(dmpe)$_2$(Cl)(NO) (**1**) and the borohydride complex Mo(η^1-BH$_4$)(dmpe)$_2$(NO) (**2**) (Scheme 1).

Reaction of *trans*-Mo(CO)$_4$(NO)(ClAlCl$_3$) with 3 equiv of dmpe in an autoclave in THF at 160 °C for 8 days produced the chloride **1** in high yield. On the basis of the fact that the analogous reaction with PMe$_3$ proceeded under milder conditions to afford trisphosphine-substituted compound,[8] the reaction with dmpe is believed to undergo first facile substitution of two or three CO groups and only under forcing conditions (high temperatures and long reaction times) is the remaining CO ligand also replaced.

Scheme 1

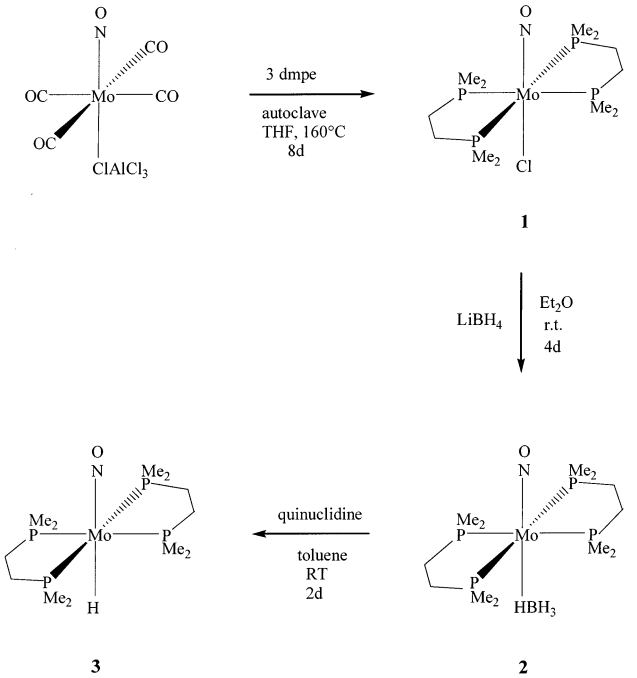

Table 1. Selected Bond Lengths [Å] and Bond Angles [deg] of 1

Mo(1)−N(1)	1.851(4)	N(1)−Mo(1)−P(2)	91.30(9)
Mo(1)−P(1)	2.4509(4)	N(1)−Mo(1)−P(1)	89.02(9)
Mo(1)−P(2)	2.4433(5)	P(2)−Mo(1)−P(1)	80.850(14)
Mo(1)−Cl(1)	2.4881(14)	P(2)−Mo(1)−Cl(1)	87.98(2)
N(1)−O(1)	1.187(4)	P(1)−Mo(1)−Cl(1)	91.08(3)
		N(1)−Mo(1)−Cl(1)	179.25(9)

The structure of complex **1** was established on the basis of IR and NMR spectroscopy, mass spectrometry, and elemental analyses. The IR spectrum in THF shows a band at 1553 cm^{-1}, which corresponds to the NO stretching vibration. The mass spectrum shows the correct molecular peak for *trans*-MoCl(dmpe)$_2$(NO)$^+$, and no higher peaks are found. The ^{1}H NMR in C$_6$D$_6$ displays a singlet at 1.35 ppm and two multiplets at 1.45 and 1.24 ppm, which are assigned to the proton resonances of the PMe and PCH$_2$ groups, respectively. The ^{31}P NMR reveals only a singlet at 35.4 ppm, indicating the chemical equivalence of the four phosphorus atoms around the molybdenum center and on this basis the trans disposition of the chloride and nitrosyl ligand.

The molecular structure of chloride **1** was then unambiguously assigned by a X-ray diffraction study. Crystals suitable for the X-ray analysis were grown by cooling a saturated diethyl ether solution of **1** to −30 °C. Selected bond distances and angles of the complex are given in Table 1. The structure is shown in Figure 1. In accordance with the spectroscopic data, complex **1** has a pseudo-octahedral structure with four phosphorus atoms in the equatorial plane and the trans-disposed nitrosyl and chloride ligands, which display disorder.

Treatment of chloride **1** with excess LiBH$_4$ in diethyl ether resulted in the conversion of **1** to the borohydride **2** (Scheme 1). The isolation of **2** proved to be troublesome. It was ulitmately accomplished by repeated extraction of the solid mixture with toluene, which

(7) (a) Kundel, P.; Berke, H. *J. Organomet. Chem.* **1987**, *335*, 353. (b) van der Zeijden, A. A. H.; Berke, H. *Helv. Chim. Acta* **1992**, *75*, 513. (c) van der Zeijden, A. A. H.; Bosch, H. W.; Berke, H. *Organometallics* **1992**, *11*, 2051. (d) van der Zeijden, A. A. H.; Veghini, D.; Berke, H. *Inorg. Chem.* **1992**, *31*, 5106. (e) van der Zeijden, A. A. H.; Berke, H. *Helv. Chim. Acta* **1992**, *75*, 513. (f) Nietlispach, D.; Bosch, H. W.; Berke, H. *Chem. Ber.* **1994**, *127*, 2403. (g) Nietlispach, D.; Veghini, D.; Berke, H. *Helv. Chim. Acta* **1994**, *77*, 2197. (h) Furno, F.; Fox, T.; Schmalle, H. W.; Berke, H. *Organometallics* **2000**, *19*, 3620. (i) Höck, J.; Jacobsen, H.; Schmalle, H. W.; Artus, G. R. J.; Fox, T.; Amor, J. I.; Bäth, F.; Berke, H. *Organometallics* **2001**, *20*, 1533. (j) Furno, F.; Fox, T.; Alfonso, M.; Berke, H. *Eur. J. Inorg. Chem.* **2001**, 1559.

(8) Liang, F.; Jacobsen, H.; Schmalle, H. W.; Fox, T.; Berke, H. *Organometallics* **2000**, *19*, 1950.

(9) Kann, C. T.; Hitchcock, P. B.; Richards, R. L. *J. Chem. Soc., Dalton Trans.* **1982**, 79.

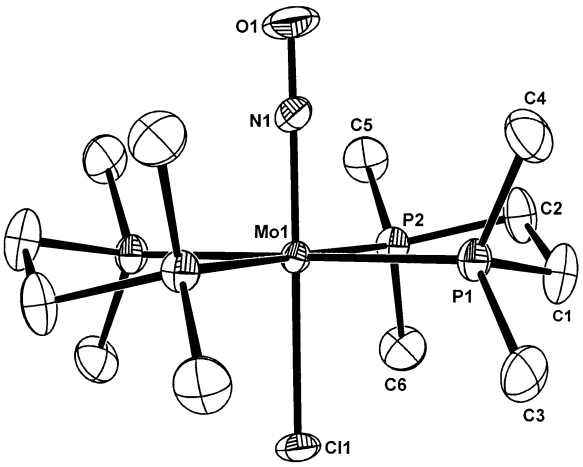

Figure 1. ORTEP plot of the structure of **1**. Displacement ellipsoids are drawn with 50% probability. Labeling for the symmetry-related atoms (sym.op.i = $-x+1, -y+1, -z$) is not shown. The hydrogen atoms have been omitted for clarity.

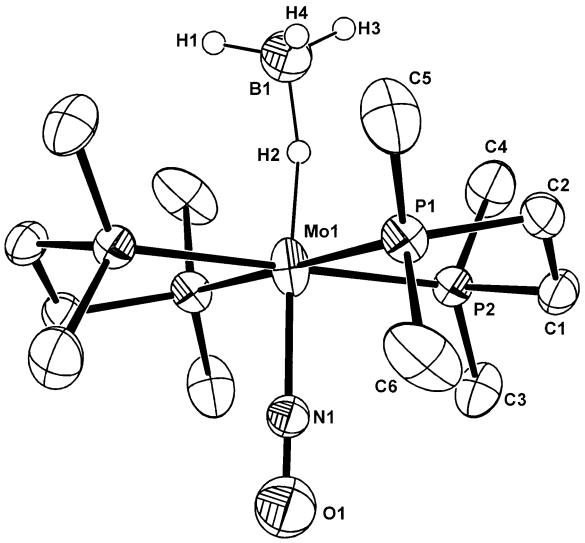

Figure 2. ORTEP plot of the structure of **2**. Displacement ellipsoids are drawn with 50% probability. Labeling for the symmetry-related atoms (sym.op.i = $-x+1, -y+1, -z$) is not shown. The hydrogen atoms except for those of BH_4 have been omitted for clarity.

provided the product in only 20−30% yield in a first batch. Redissolution of the residue in diethyl ether and cooling of the resulting solution to −30 °C overnight and then removal of the diethyl ether and extraction again with toluene afforded further product. For a better overall yield, it was necessary to repeat this inconvenient and time-consuming separation procedure four to five times. It can be inferred that the difficulty of the isolation of **2** originates from the formation of higher lithium borohydride adducts, which in diethyl ether partly release **2** in equilibrium quantities as demonstrated by eq 1:

$$[\textit{trans}\text{-Mo(dmpe)}_2(HBH_3)(NO)]_x[LiBH_4]_y \rightleftharpoons x\,[\textit{trans}\text{-Mo(dmpe)}_2(HBH_3)(NO)] + y\,LiBH_4 \quad (1)$$

The lithium borohydride-enriched species are apparently insoluble in toluene, which allows the extraction of **2** from a solid equlibrium mixture with this solvent. It may be invoked that it is the coordination ability of the nitrosyl group that promotes formation of these adduct. $LiBH_4$ or $Li[HBR_3]$ forms related adducts with the chloride **1**, as well as with the hydride **3**.[10]

In the ^1H NMR spectrum in C_6D_6 **2** shows a characteristic broad quartet at −2.26 ppm with a ^{11}B coupling constant of $^1J_{HB} = 81$ Hz, which corresponds to the proton resonance of the tetrahydroborate group. The signal does not reveal further splitting at −60 °C in C_7D_8, indicating a fast exchange process between the bridging and nonbridging H atoms of the BH_4 group even at low temperature. In C_6D_6 two singlets at 1.40, 1.26 ppm and two multiplets at 1.47, 1.19 ppm are assigned to the resonances of the PMe and PCH_2 group protons, respectively. The ^{31}P NMR spectrum in C_6D_6 displays a singlet at 36.2 ppm, corresponding to the four chemically equivalent phosphorus atoms of the phosphine ligands. In contrast to the previously reported borohydride Mo(η^1-BH_4)(CO)(NO)$(PMe_3)_3$[8] and other boron-containing compounds,[11] sharp signals of the proton and phosphorus resonances were observed, despite the interference of the ^{11}B quadrupolar relaxation, which normally causes broadening. The observation of a quintet at −42.1 ppm ($^1J_{HB} = 81$ Hz) in the ^{11}B NMR spectrum additionally confirms the presence of the tetrahydroborate group in the molecule.

Table 2. Selected Bond Lengths [Å] and Bond Angles [deg] of 2

Mo(1)−N(1)	1.966(5)	N(1)−Mo(1)−P(2)	87.72(14)
Mo(1)−P(1)	2.4569(7)	N(1)−Mo(1)−P(1)	91.78(15)
Mo(1)−P(2)	2.4512(7)	P(2)−Mo(1)−P(1)	80.62(2)
N(1)−O(1)	1.172(9)	Mo(1)−H(2)−B(1)	150(6)
Mo(1)−H(2)	1.66(5)	N(1)−Mo(1)−H(2)	167(3)

By cooling a saturated diethyl ether solution of **2** to −30 °C overnight crystals suitable for an X-ray diffraction study were obtained. A model of **2** is displayed in Figure 2. Although there is disorder of the nitrosyl and BH_4 groups, the η^1-binding mode of the BH_4 unit in **2** is unambiguously established. This feature is similar to that in Mo(η^1-BH_4)(CO)(NO)$(PMe_3)_3$, and it is thought to be enforced by the residual ligand sphere providing sufficient electronic saturation to the metal center. The Mo−N and Mo−H_{BH4} bond distances of **2** (Table 2) are apparently different from those of Mo(η^1-BH_4)(CO)(NO)-$(PMe_3)_3$. However, any definite structural comparison of these complexes, e.g., the influence of the phosphine donors on the binding strengths of the nitrosyl and BH_4 groups, is precluded by the inaccuracy of the structural data due to the disorder of NO and BH_4 units.

Conversion of the borohydride complexes into the corresponding hydride compounds is accomplished by the reaction with Lewis bases to remove BH_3. As in the case of the conversion of Mo(η^1-BH_4)(CO)(NO)$(PMe_3)_3$,[8] we have tried to use trimethylphosphine as a borane scavenger. But PMe_3 turned out to be less effective in the case of **2**. Only 50% conversion of the borohydride **2** was observed after 4 days employing even up to 15 equiv of PMe_3 in toluene at room temperature. Alternatively, quinuclidine can be used.[4h,7h]

Treatment of **2** with 8 equiv of quinuclidine in toluene at room temperature for 2 days produced the desired

(10) Liang, F. Ph.D. Thesis, University of Zurich, 2001.
(11) (a) Beall, H.; Bushweller, C. H. *Chem. Rev.* **1973**, *73*, 465. (b) Marks, T. J.; Kolb, J. R. *Chem. Rev.* **1977**, *77*, 263.

hydride **3**. The removal of the $R_3N \rightarrow BH_3$ byproducts and the excess of quinuclidine was achieved by extraction of the reaction mixture with pentane and subsequent sublimation of the impurities at 60 °C in vacuo. The hydride **3** was finally isolated in yields over 90%.

In the IR spectrum of **3** in THF the NO stretching vibration was found at 1557 cm^{-1}. Similar to the case of *mer*-Mo(CO)(H)(NO)(PMe_3)$_3$, the Mo−H bond vibration of **3** could not be observed. The ^{1}H NMR of **3** in C_6D_6 shows besides the proton resonances of the PMe and PCH_2 groups a quintet at −4.58 ppm due to the coupling with the four chemically equivalent phosphorus nuclei ($^2J_{HP} = 29$ Hz). Compared with the corresponding hydride resonance of *mer*-Mo(CO)(H)(NO)(PMe_3)$_3$ (−1.92 ppm), that of **3** appears at relatively high field. The ^{31}P NMR spectrum displays a singlet at 44.2 ppm.

Ionicities of the Mo−D bonds of *trans*-Mo(dmpe)$_2$(D)(NO) (3a) and *mer*-Mo(CO)−(D)(NO)(PMe_3)$_3$ (4). Our group has previously reported the determination of bond ionicities (*i*) of a series of transition metal deuterides via the T_{1min} measurements of the ^{2}H nucleus in solution and used the bond ionicity as an indicator of the hydridic character of the L_nM-H bond.[6] For this the deuterides *trans*-Mo(dmpe)$_2$(D)(NO) (**3a**) and *mer*-Mo(CO)(D)(NO)(PMe_3)$_3$ (**4**) had to be prepared.

3a and **4** were synthesized analogously to the corresponding H compounds. An equimolar mixture of $NaBD_4$ and LiCl was used as a substitute for $LiBH_4$ in the conversions of the chlorides to the borohydrides. The ^{2}H NMR T_1 relaxation times for both deuterides have been measured in toluene-h_8 at different temperatures, which resulted in values of T_{1min} of 53 and 48 ms for **3a** and **4**, respectively. Accordingly, the deuterium quadrupole coupling constants (DQCCs) were calculated to be 36 ± 1 and 38 ± 1 kHz, and the ionicities of the Mo−D(H) bonds are 84.1 ± 0.5% and 83.3 ± 0.5% for **3a** and **4**, respectively. These bond ionicity values are significantly larger than those reported previously for related nitrosyl-substituted transition metal deuterides[6] such as Re(CO)D_2(NO)(PMe_3)$_2$ and W(CO)$_2$D(NO)(PMe_3)$_2$, spanning a range from 69% to 76%, and they are close to the value of 86% for LiD.[12] This stresses the strong polarity of the Mo−D bond in both complexes. These highly polar characters for the Mo−D bonds in **3a** and **4** may be attributed to the electronic effects of the ligand sphere, specifically to the electron-donating property of the phosphines and to the trans influence of the nitrosyl group. The bond ionicity of **3a** is somewhat larger than that of **4,** which, if significant, may reflect the higher number of phosphine substitutents.

In addition the DQCCs of **3a** and **4** were determined by the rarely used solid-state ^{2}H NMR method. The following correlation is valid:[13]

$$\mathrm{DQCC} = (4/3)I\Delta(1-\eta)$$

where *I* is the nuclear spin of the ^{2}H nucleus, Δ is defined as the distance between the two outer signals in the solid-state ^{2}H NMR spectrum, and η is the asymmetry parameter of the electrical field. In an isotropic solid system η would be zero. The VT solid-state ^{2}H NMR spectra of **3a** and **4** are presented in Figure 3. From the spectra the Δ values of 36 and 39 kHz are obtained, DQCCs are calculated amounting to 48 ± 0.2 and 52 ± 0.2 kHz, and the bond ionicity *i* values are 78.8 ± 0.1% and 77.1 ± 0.1% for **3a** and **4**, respectively. The results indicate again that the hydridic polarization of the Mo−D bond is stronger in **3a** than in **4**. However, the DQCCs of both complexes **3a** and **4** obtained from the measurements in solution are smaller than those determined in the solid state. A similar situation has been observed for W(CO)(D)(NO)(PMe_3)$_3$.[14] This difference is probably due to an electrical field anisotropy in the solid state. Since the two peaks of the "Pake doublet"[13] are broadened and the outside line components are not observable due to strong dipolar interactions with the neighboring ^{31}P nuclei, it was not possible to use simulation techniques to correct for the anisotropy.

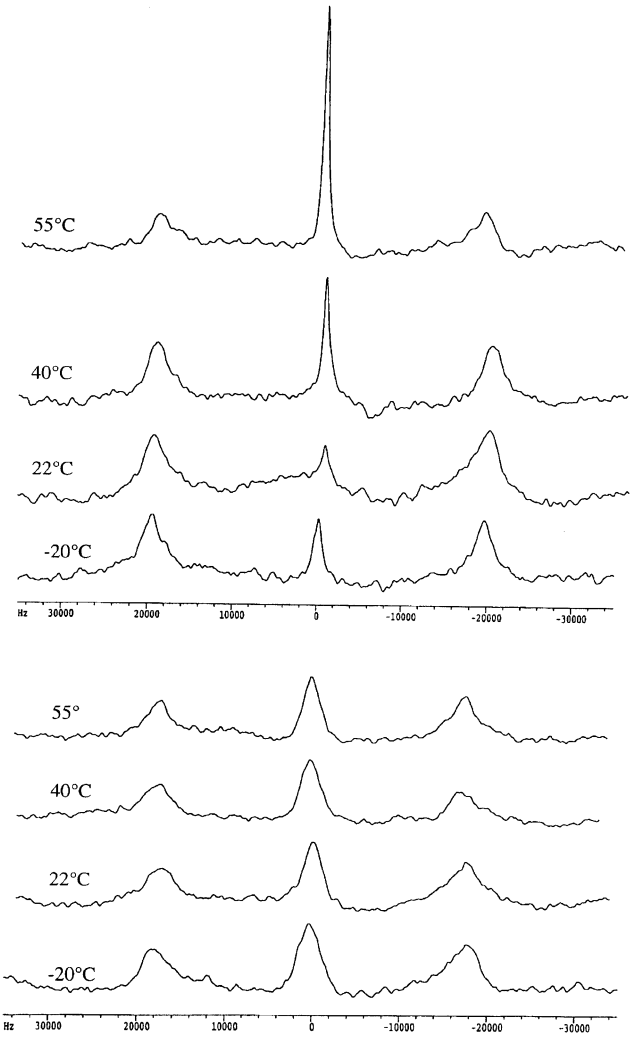

Figure 3. Static solid-state ^{2}H NMR spectra of **4** (above) and **3a** (below) at various temperatures. The chemical shift (Hz) of the center resonance has been arbitrarily set to zero.

It is noteworthy that the solid-state ^{2}H NMR of **3a** and **4** display unexpected temperature dependencies in the range −20 to +50 °C (Figure 3). For **4** a singlet resonance can be observed at high temperature (55 °C), while at low temperature (−20 °C), this resonance

(12) Wharton, L.; Gold, L. P.; Klemperer, W. *J. Chem. Phys.* **1962**, *37*, 2149.
(13) Fyfe, C. A. *Solid State NMR for Chemists;* CFC Press: Guelph, 1983.
(14) Höck, J. Ph.D. Thesis, University of Zurich, 2001.

becomes very weak and is replaced by the expected "Pake doublet". Such temperature dependence of the solid-state ^{2}H NMR spectra is similar to that observed for W(CO)(D)(NO)(PMe_3)$_3$[14] and W(≡CMes)(D)(dmpe)$_2$,[15] where the singlet resonance even fully disappeared at low temperature (−30 and −40 °C, respectively). This phenomenon is believed to result from ^{2}H mobility in the solid state of **4**. The solid-state ^{2}H NMR spectrum of **3a** displays a singlet over the whole available temperature range. This is again interpreted in terms of exchange and consequently mobility of the D ligand, however, apparently occurring with an even lower barrier than for **4**. Although the observation is new and a mechanism not yet available, it seems to be a general characteristic for hydridic hydrides. Further detailed work has to be carried out to trace the real cause and the mechanism of this mobility behavior.

Reactivity of *trans*-Mo(dmpe)$_2$(H)(NO) (3). Considering the high reactivity of the hydride *mer*-Mo(CO)(H)(NO)(PMe_3)$_3$[8] and its high hydridic character of the Mo−H bond, we may anticipate that the activity of such hydrides parallels their hydridicity. The fact that hydride **3** possesses an even enhanced hydridic Mo−H bond led us to suspect that **3** would show an increased propensity to undergo hydride transfer reactions. Therefore, it was of great interest to test the insertion capabilities of **3**. Furthermore, insertion reactions of metal hydrides are of fundamental importance, representing key steps in many catalytic transformations of unsaturated substrates with transition metal compounds.[16] In this study simple ketones and metal carbonyl compounds were chosen as relatively polar substrates, since they were supposed to react with a relatively greater ease with polar hydride transfer agents.

Reactions of **3** with benzophenone, acetophenone, and acetone were completed in 2, 1.5, and 3 h, respectively, under otherwise mild conditions to afford the corresponding alkoxide complexes *trans*-Mo(dmpe)$_2$(NO)(OCHRR′) (R = R′ = Ph (**5**); R = Me, R′ = Ph (**6**); R = R′ = Me (**7**)). The reaction times are short compared with the corresponding ones of *mer*-Mo(CO)(H)(NO)(PMe_3)$_3$ (3, 7, 10 h for Ph_2CO, PhCOMe, Me_2CO, respectively) (Scheme 2). In contrast to the case of *mer*-Mo(CO)(H)(NO)(PMe_3)$_3$, the reaction times of **3** with the three ketones vary only little in dependence of the electrophilic character of the $C_{carbonyl}$ atom. This lower selectivity is presumably due to the fact that **3** is a "hotter" species and the whole reaction profile more exothermic so that the ability for kinetic distinction is greatly reduced.

The alkoxide complexes **5**, **6**, and **7** have been fully characterized by elemental analysis, MS, IR, and NMR

Scheme 2

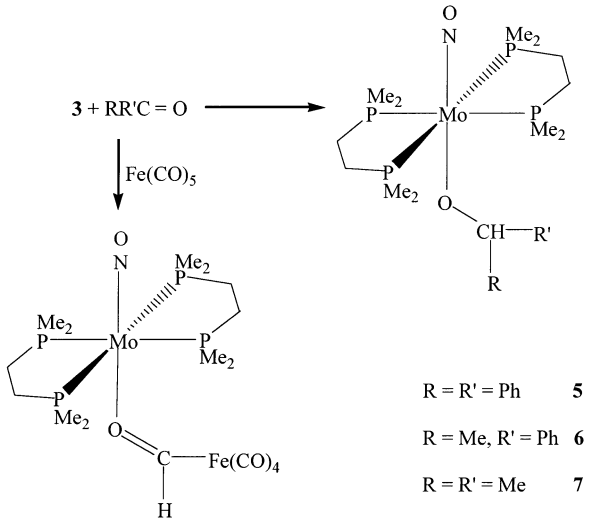

spectroscopy. The ^{1}H NMR spectrum of **5** in C_6D_6 shows among other resonances a characteristic singlet at 5.03 ppm, which corresponds to the proton resonance of the newly formed −CH− moiety. In the ^{13}C NMR spectrum the characteristic resonance for this carbon atom appears at 85.3 ppm as a quintet signal. The splitting of the signal results from the coupling with the four phosphorus nuclei. The newly formed −CH− moiety for **6** appears in the ^{1}H NMR spectrum at 4.14 ppm split into a quartet signal due to coupling with the methyl group. The resonance of the respective carbon atom was observed as a quintet at 77.5 ppm in the ^{13}C NMR spectrum. The methyl groups of the dmpe ligands of **6** are diastereotopic due to the chiral center at the carbon, which causes two sets of multiplets in the ^{1}H NMR spectrum at 1.30 and 1.22 ppm. This diastereotopy is also reflected in the ^{31}P{^{1}H} NMR spectrum, where not the expected singlet but a symmetric higher order multiplet is observed at 32.4 ppm. For complex **7** the ^{1}H NMR displays also a characteristic heptet resonance at 3.25 ppm for the newly formed −CH− moiety. The ^{13}C{^{1}H} NMR shows for this CH group a quintet at 69.3 ppm.

Treatment of **3** with 1 equiv of Fe(CO)$_5$ in toluene at room temperature afforded the formyl-bridged complex *trans*-Mo(dmpe)$_2$(NO)[(μ-OCH)Fe(CO)$_4$] (**8**) in a few minutes (Scheme 2). **8** was found to be insoluble in pentane, sparingly soluble in toluene, and soluble in THF. After diffusion of pentane into a concentrated THF solution the complex was isolated as orange crystals in 81% yield. The IR spectrum of **8** in THF displays three bands at 2032, 1949, and 1918 cm^{-1} attributed to ν(CO) vibrations of the Fe(CO)$_4$ moiety. These spectroscopic data are very similar to those of the analogous complex *mer*-Mo(CO)(NO)(PMe_3)$_3$[(μ-OCH)Fe(CO)$_4$][8] and the "parent" [Fe(CO)$_4$CHO]$^-$ anion.[17] In the ^{1}H NMR spectrum of **8** (C_6D_6) the characteristic proton resonance of the bridging formyl group appears at 13.52 ppm as a singlet. In the ^{13}C{^{1}H} NMR spectrum the resonance for the carbon atom of this bridging formyl group is observed at 299.3 ppm as a quintet.

(15) Furno, F. Ph.D. Thesis, University of Zurich, 2001.

(16) Selected references: (a) Gladysz, J. A. *Adv. Organomet. Chem.* **1982**, *20*, 1. (b) Blackborow, J. R.; Daroda, R. J.; Wilkinson, G. *Coord. Chem. Rev.* **1982**, *43*, 17. (c) Darensbourg, D. J.; Kudaroski, R. A. *Adv. Organomet. Chem.* **1983**, *22*, 129. (d) Costa, L. C. *Catal. Rev. Sci. Eng.* **1983**, *25*, 325. (e) Dombek, B. P. *Adv. Catal.* **1983**, *32*, 325. (f) Noyori, R.; Takaya, H. *Acc. Chem. Res.* **1990**, *23*, 345. (g) Klingler, R. J.; Rathke, J. W. *Prog. Inorg. Chem.* **1991**, *39*, 113. (h) Süss-Fink, G.; Meister, G. *Adv. Organomet. Chem.* **1993**, *35*, 41. (i) Miller, R. L.; Toreki, R.; La Pointe, R. E.; Wolczanski, P. T.; Van Duyne, G. D.; Roe, D. C. *J. Am. Chem. Soc.* **1993**, *115*, 5570. (j) Simpson, M. C.; Cole Hamilton, D. J. *Coord. Chem. Rev.* **1996**, *155*, 163. (k) Gibson, D. H. *Chem. Rev.* **1996**, *96*, 2063. (l) Burk, M. J.; Gross, M. F.; Harper, T. G. P.; Kalberg, C. S.; Lee, J. R.; Martinez, J. P. *Pure Appl. Chem.* **1996**, *68*, 37. (m) Nomura, K. *J. Mol. Catal. A: Chem.* **1998**, *130*, 1. (n) Palmer, M. J.; Wills, M. *Tetrahedron: Asymmetry* **1999**, *10*, 2045.

(17) Collman, J. P.; Winter, S. R. *J. Am. Chem. Soc.* **1973**, *95*, 4089.

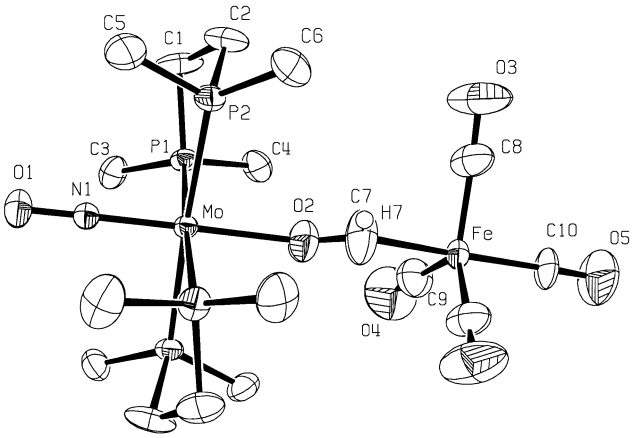

Figure 4. ORTEP plot of the structure of **8**. Displacement ellipsoids are drawn with 50% probability. Labeling for symmetry-related atoms is not shown (sym. op. i = $-x+2$, y, z). The hydrogen atoms, except H7, have been omitted for clarity.

Table 3. Selected Bond Lengths [Å] and Bond Angles [deg] of 8

Mo−N(1)	1.791(5)	N(1)−Mo−P(2)	91.18(12)
Mo−O(2)	2.188(6)	N(1)−Mo−P(1)	91.32(12)
Mo−P(1)	2.4646(11)	P(2)−Mo−P(1)	80.35(4)
Mo−P(2)	2.4677(11)	O(2)−Mo−P(1)	87.30(12)
N(1)−O(1)	1.205(7)	O(2)−Mo−P(2)	90.20(12)
C(7)−O(2)	1.119(12)	C(7)−O(2)−Mo	145.7(8)
Fe−C(7)	1.953(11)	O(2)−C(7)−Fe	136.3(10)

Crystals suitable for X-ray diffraction analysis of **8** were obtained by diffusion of pentane into a THF solution of the complex. The molecular structure of **8** is shown in Figure 4. The complex reveals an octahedral coordination around the molybdenum center, which is very similar to those of complexes **1** and **2**. The coordination around the iron center is pseudo-trigonal bipyramidal. Both the Mo−N(1) and Mo−O(2) distances (Table 3, 1.791(5) and 2.188(6) Å, respectively) of **8** are only a little longer (about 0.015 Å) than the corresponding distances in complex *mer*-Mo(CO)(NO)(PMe_3)$_3$[(μ-OCH)Fe(CO)$_4$],[8] suggesting similar binding strengths of the nitrosyl and the bridging formyl groups in both species. The C(7)−O(2)−Mo angle of 145.7(8)° and the O(2)−C(7)−Fe angle of 136.3(10)° in **8** are comparable to the corresponding ones in *mer*-Mo(CO)(NO)(PMe_3)$_3$-[(μ-OCH)Fe(CO)$_4$], indicating only marginal influence of the different phosphine environments of both compounds.

Reaction of **3** with 1 equiv of $Re_2(CO)_{10}$ in toluene proceeded to completion at room temperature with formation of the corresponding formyl-bridged complex *trans*-Mo(dmpe)$_2$(NO)[(μ-OCH)Re_2(CO)$_9$] (**9**). The reaction was over in a few minutes, and the product was isolated as orange crystals in 86% yield. In the ^{1}H NMR spectrum of **9** (in C_6D_6) the characteristic resonance of the formyl proton is observed as a singlet at 14.57 ppm. The ^{13}C{^{1}H} NMR displays a multiplet at 298.4 ppm for the resonance of the formyl carbon atom.

Diffusion of pentane into a concentrated toluene solution of complex **9** gave crystals suitable for an X-ray diffraction study. As shown in Figure 5 the molybdenum center in **9** adopts a pseudo-octahedral geometry as in the series of complexes **1**, **2**, and **8**. The geometry of the [Re_2(CO)$_9$CHO] fragment is grossly similar to that of

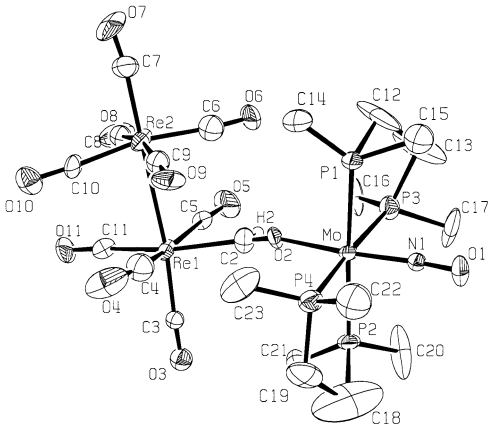

Figure 5. ORTEP plot of the structure of **9**. Displacement ellipsoids are drawn with 50% probability. The hydrogen atoms, except H2, have been omitted for clarity.

Table 4. Selected Bond Lengths [Å] and Bond Angles [deg] of 9

Mo−N(1)	1.781(8)	N(1)−Mo−P(1)	88.9(3)
Mo−O(2)	2.258(8)	N(1)−Mo−P(2)	88.5(3)
Mo−P(1)	2.466(2)	N(1)−Mo−P(3)	82.5(3)
Mo−P(2)	2.454(3)	N(1)−Mo−P(4)	94.7(3)
Mo−P(3)	2.542(5)	N(1)−Mo−O(2)	164.1(4)
Mo−P(4)	2.407(5)	P(1)−Mo−P(3)	80.1(2)
N(1)−O(1)	1.200(12)	P(4)−Mo−P(2)	80.7(2)
C(2)−O(2)	0.914(15)	O(2)−C(2)−Re(1)	169.2(13)
Re(1)−C(2)	2.180(14)	C(2)−O(2)−Mo	164.8(11)

the analogous complexes bearing the formyl groups in equatorial positions.[8,18] The Mo−N(1) distance of 1.781-(8) Å of complex **9** (Table 4) does not reveal a significant difference compared to the corresponding distance of the previously reported complex *mer*-Mo(CO)(NO)(PMe_3)$_3$-[(μ-OCH)Re_2(CO)$_9$] (1.772(6) Å);[8] however the Mo−O(2) distance of 2.258(8) Å and the Re(1)−C(2) distance of 2.180(14) Å in **9** are much longer than those in the related complex bearing PMe_3 ligands (2.173(5) and 2.102(7) Å, respectively). This indicates greater steric repulsion at the level of a higher degree of phosphine substitution. This influence is also reflected in the bond angles of the Mo−O−C−Re bridge. In the complex *mer*-Mo(CO)(NO)(PMe_3)$_3$[(μ-OCH)Re_2(CO)$_9$], the C(11)−O(3)−Mo angle (127.8(5)°) and the O(3)−C(11)−Re(1) angle (127.5(5)°) show much greater bends than those of complex **9** (Table 4, corresponding bond angles are 164.8(11)° and 169.2(13)°). It is assumed that the difference arises from steric factors. Again in complex **9** there is greater steric crowding of the dmpe ligands, which prevents the Mo(dmpe)$_2$(NO) fragment to come closer to the Re_2(CO)$_9$ unit.

The hydride transfer reaction of **3** with Fe(CO)$_5$ did not show fundamental deviations from that of *mer*-Mo-(CO)(H)(NO)(PMe_3)$_3$.[8] Both reactions proceeded rapidly to completion at room temperature. In contrast to this, the reactions of both hydrides with $Re_2(CO)_{10}$ are significantly different. While the reaction of *mer*-Mo-(CO)(H)(NO)(PMe_3)$_3$ with $Re_2(CO)_{10}$ establishes an equilibrium, the corresponding reaction of **3** proceeded to completion, which reflects a less activated Mo−H bond for **3**. More interestingly, further reaction of complex **9** with **3** established double insertion of **3** into $Re_2(CO)_{10}$.

(18) Casey, C. P.; Neumann, S. M. *J. Am. Chem. Soc.* **1978**, *100*, 2544.

Scheme 3

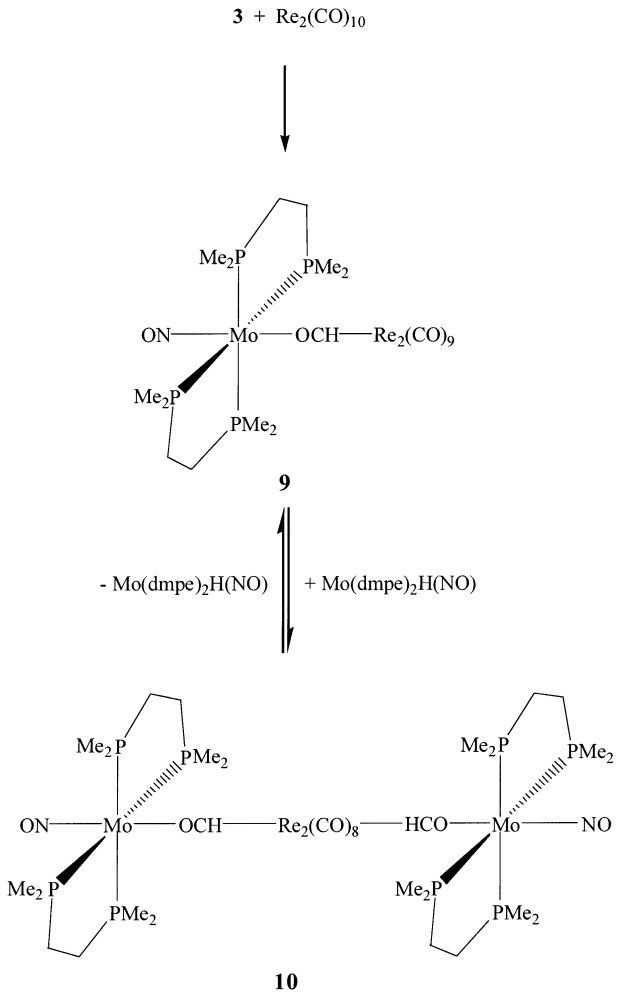

Even in the ^{1}H NMR spectrum of the equimolar mixture of **3** and $Re_2(CO)_{10}$ (in C_7D_8) a new singlet appeared at 14.66 ppm besides the signal at 14.57 ppm for the formyl group of **9**, suggesting the formation of the new compound **10**, also bearing formyl groups. In the $^{31}P\{^1H\}$ spectrum of the same mixture a new singlet was observed at 36.5 ppm besides the signals of **3** and **9**, confirming further the existence of a new species. We assume that the new compound **10** is the product of a second insertion reaction of **3** with **9**. The observations of the coexistence of the signals corresponding to **3**, **9**, and the new complex **10** in the mixture of all these constituents and the temperature-dependence of the integrals of these signals indicate that the subsequent transformation of **3** with **9** is a reversible process (Scheme 3). The occurrence of an equilibrium was confirmed by a 1D-EXSY experiment. When the hydride signal of **3** at −4.72 ppm was irradiated, apparent exchange of the signals at 14.57 and 14.66 ppm (resonances for the formyl protons of **9** and **10**, respectively) was clearly indicated (Figure 6).

The equilibrium constant K of the reaction of **3** with **9** shown in Scheme 3 has been determined by NMR spectroscopy in THF-d_8 at variable temperatures. At 298 K the K value was 1.99 L/mol, indicating that the equilibrium lies mainly to the left side of the reaction. From the van't Hoff plot depicted in Figure 7, ΔH and ΔS were calculated to be -58.8 ± 2.7 kJ·mol^{-1} and -48 ± 2 J·K^{-1}·mol^{-1}. The ΔH value indicates that the reaction is moderately exothermic, which apparently can be related to the relatively weak Mo−H bond of **3**, and the quite negative entropy value speaks for the associative nature of the reaction.

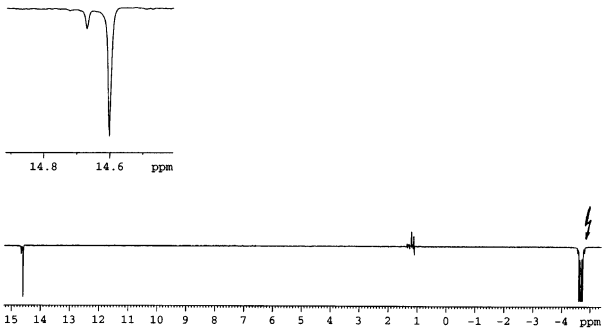

Figure 6. 1D-EXSY spectrum of the reaction mixture in Scheme 2 (C_7D_8, 333 K).

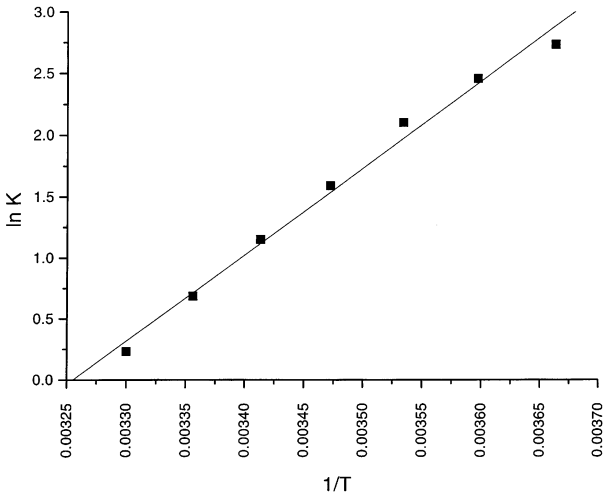

Figure 7. Van't Hoff plot for the equilibrium reaction of **9** with **3** to give **10** as shown in Scheme 3. ΔH and ΔS values are given in the text.

Due to the equilibrium reaction depicted in Scheme 3, **10** could not be isolated as an analytically pure sample, since **10** tends to cocrystallize with **9**, thus impeding its full characterization by IR, NMR spectroscopy, and elemental analysis. But the molecular structure of **10** has been established unambiguously by single-crystal X-ray diffraction. A few crystals suitable for this study were obtained by diffusion of pentane into a concentrated toluene mixture containing **9** with 4 equiv of **3**. Under these conditions complex **10** crystallized as a toluene solvate. An ORTEP drawing of **10** is given in Figure 8. For clarity the toluene solvate molecule is omitted. Selected bond distances and angles are given in Table 5. The structure shows clearly that insertions of two molecules of **3** into one $Re_2(CO)_{10}$ occurred. Each $Re(CO)_5$ unit of $Re_2(CO)_{10}$ bears one inserted hydride molecule, and the two units are arranged in an anti-conformation. Both of the bridging formyl groups are located in equatorial positions of the $Re(CO)_5$ moieties. The corresponding bond lengths and angles of the two Re−C−O−Mo bridges of the formyl groups are almost equal, and in contrast to the situation of complex **9**, they do not show great differences when compared with those of the corresponding bond lengths and angles of *mer*-$Mo(CO)(NO)(PMe_3)_3[(\mu\text{-}OCH)Re_2(CO)_9]$, indicating in this case only minor stereoelec-

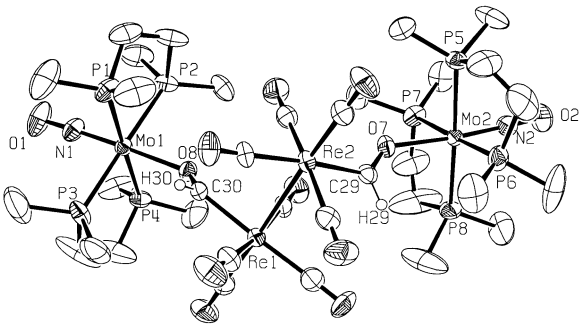

Figure 8. ORTEP plot of the structure of **10**. Displacement ellipsoids are drawn with 50% probability. The hydrogen atoms, except H29 and H30, have been omitted for clarity.

Table 5. Selected Bond Lengths [Å] and Bond Angles [deg] of 10

Mo(1)−N(1)	1.782(7)	N(1)−Mo(1)−P(1)	89.2(3)
Mo(1)−O(8)	2.207(5)	N(1)−Mo(1)−P(2)	92.7(3)
Mo(1)−P(1)	2.449(2)	N(1)−Mo(1)−P(3)	87.5(3)
Mo(1)−P(2)	2.458(2)	N(1)−Mo(1)−P(4)	91.5(2)
Mo(1)−P(3)	2.465(2)	N(1)−Mo(1)−O(8)	176.6(3)
Mo(1)−P(4)	2.463(2)	P(1)−Mo(1)−P(2)	80.69(9)
N(1)−O(1)	1.212(10)	P(4)−Mo(1)−P(3)	80.00(8)
C(30)−O(8)	1.230(10)	O(8)−C(30)−Re(1)	127.6(6)
Re(1)−C(30)	2.140(8)	C(30)−O(8)−Mo(1)	134.5(5)
Mo(2)−N(2)	1.771(7)	N(2)−Mo(2)−P(5)	90.5(2)
Mo(2)−O(7)	2.194(5)	N(2)−Mo(2)−P(6)	89.5(3)
Mo(2)−P(5)	2.457(2)	N(2)−Mo(2)−P(7)	90.7(3)
Mo(2)−P(6)	2.467(2)	N(2)−Mo(2)−P(8)	90.6(2)
Mo(2)−P(7)	2.444(2)	N(2)−Mo(2)−O(7)	175.4(3)
Mo(2)−P(8)	2.449(2)	P(5)−Mo(2)−P(6)	80.22(8)
N(2)−O(2)	1.223(10)	P(7)−Mo(2)−P(8)	80.87(8)
C(29)−O(7)	1.251(10)	O(7)−C(29)−Re(2)	127.8(6)
Re(2)−C(29)	2.132(8)	C(29)−O(7)−Mo(2)	135.8(5)

tronic influences of the dmpe ligands on the structure of the formyl group. The reasons for this remain to be explained.

It was of further interest to extend the study to the reaction of **3** with $Mn_2(CO)_{10}$,[19] which displays a weaker metal−metal bond and therefore was expected to show a different reaction pattern. The reaction of **3** with equimolar amounts of $Mn_2(CO)_{10}$ was carried out in C_7D_8 and monitored by NMR spectroscopy. From the time-dependent ^1H and $^{31}P\{^1H\}$ NMR spectra of the reaction mixture, one could see that **3** was consumed in a few minutes to yield the new compound *trans*-Mo(dmpe)$_2$(NO)[(μ-OCH)Mn$_2$(CO)$_9$], **11**, in analogy with the reaction with $Re_2(CO)_{10}$ (Scheme 4). However, in contrast to **9**, **11** was quite unstable and decomposed into another complex, *trans*-Mo(dmpe)$_2$(NO)[(μ-OC)Mn(CO)$_4$] (**12**) within 2 days. Attempts to isolate and further characterize complex **11** were unsuccessful. The mechanism for the conversion of **11** into **12** could not fully be traced. A mechanistic scheme is suggested in accord with that found by J. A. Gladysz et al.[25] for the cleavage of $Mn_2(CO)_{10}$ by $LiHB(C_2H_5)_3$ Superhydride (Scheme 4). Via the intermediacy of $HMn(CO)_5$, $Mn(CO)_5^-$ and H_2 are formed. H_2 also evolves from the reaction according to Scheme 4 (signal at 4.45 ppm), which is found to be accelerated in the presence of an excess of **3**. This may imply that in **11** $Mn(CO)_5^-$ acts first as a leaving group and then as a weak base. Subsequently **12** and the acidic hydride $HMn(CO)_5$ are formed. The latter then

Scheme 4

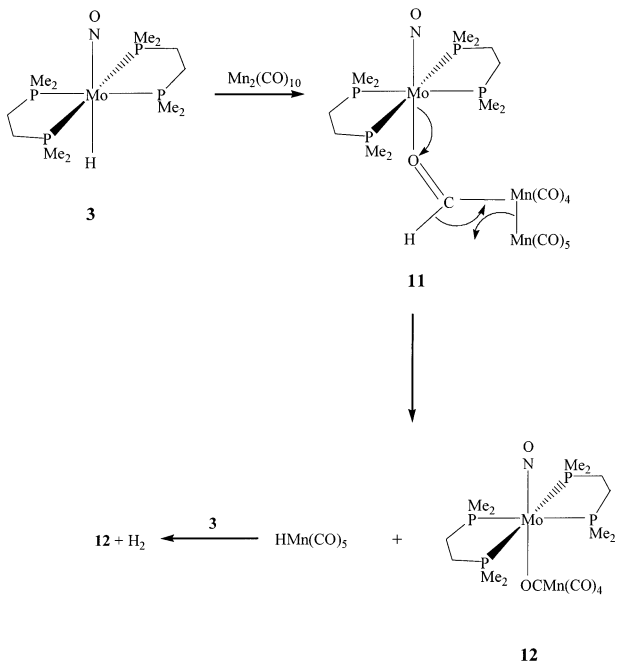

attacks the hydridic species **3** to again deliver **12** and H_2, and this step is assumed to be faster the higher the concentration of **3** is. The involvement of $HMn(CO)_5$ was probed in a separate experiment and was found to react readily with **3** in the proposed fashion. This provides evidence that especially the last step of Scheme 4 is based on realistic grounds.

In the ^1H NMR spectrum (C_7D_8, room temperature) **11** revealed a characteristic singlet at 13.51 ppm assigned to the formyl proton. A singlet at 33.9 ppm in the $^{31}P\{^1H\}$ NMR spectrum belongs to the phosphorus nuclei of **11**. Compound **12** was isolated from the reaction mixture as analytically pure, yellow crystals in 73% yield. The ^1H NMR of **12** in C_6D_6 displays two multiplets at 1.21, 1.02 ppm and two singlets at 1.16, 1.07 ppm, which can be assigned to the resonances of the CH_2 and CH_3 groups of the dmpe ligands. The $^{31}P\{^1H\}$ NMR in C_6D_6 merely shows a singlet at 36.0 ppm. In the $^{13}C\{^1H\}$ NMR spectrum a quintet at 29.1 ppm and a multiplet at 14.3 ppm were observed for the C nuclei of the dmpe ligands, and furthermore multiplets

(19) Meyer, T. J. *Prog. Inorg. Chem.* **1975**, *19*, 1.

(20) Darensbourg, M. Y.; Darensbourg, D. J.; Burns, D.; Drew, D. A. *J. Am. Chem. Soc.* **1976**, *98*, 3127.

(21) Horwitz, C. P.; Shriver, D. F. *Adv. Organomet. Chem.* **1984**, *23*, 219.

(22) (a) Schneider, M.; Weiss, E. *J. Organomet. Chem.* **1976**, *121*, 365. (b) Tilley, T. D.; Andersen, R. A. *J. Chem. Soc., Chem. Commun.* **1981**, 985. (c) Marsella, J. A.; Huffmann, J. C.; Caulton, K. G.; Longato, B.; Norton, J. R. *J. Am. Chem. Chem.* **1982**, *104*, 6360. (d) Merola, J. S.; Gentile, R. A.; Ansel, G. B.; Modrick, M. A.; Zenta, S. *Organometallics* **1982**, *1*, 1731. (e) Merola, J. S.; Campo, K. S.; Gentile, R. A.; Modrick, M. A.; Zenta, S. *Organometallics* **1984**, *3*, 334. (f) Sartain, W. J.; Selegue, J. P. *Organometallics* **1984**, *3*, 1922. (g) Boncella, J. M.; Andersen, R. A. *Inorg. Chem.* **1984**, *23*, 432. (h) Osborne, J. H.; Rheingold, A. L.; Trogler, W. C. *J. Am. Chem. Soc.* **1985**, *107*, 6292.

(23) Hamilton, D. M.; Willis, W. S.; Stucky, G. D. *J, Am. Chem. Chem.* **1981**, *103*, 4255.

(24) (a) Clegg, W.; Wheatley, P. J. *J. Chem. Soc. A* **1971**, 3572. (b) Frenz, B. A.; Ibers, J. A. *Inorg. Chem.* **1972**, *11*, 1109. (c) Katacher, M. L.; Simon, G. L. *Inorg. Chem.* **1972**, *11*, 1651. (d) Clegg, W.; Wheatley, P. J. *J. Chem. Soc., Dalton Trans.* **1973**, 90; **1974**, 424. (e) Herberhold, M.; Wehrmann, F.; Neugebauer, D.; Huttner, G. G. *J. Organomet. Chem.* **1978**, *152*, 329.

(25) Gladysz, J. A.; Williams, G. M.; Tam, W.; Johnson, D. L. *J. Organomet. Chem.* **1977**, *140*, C1.

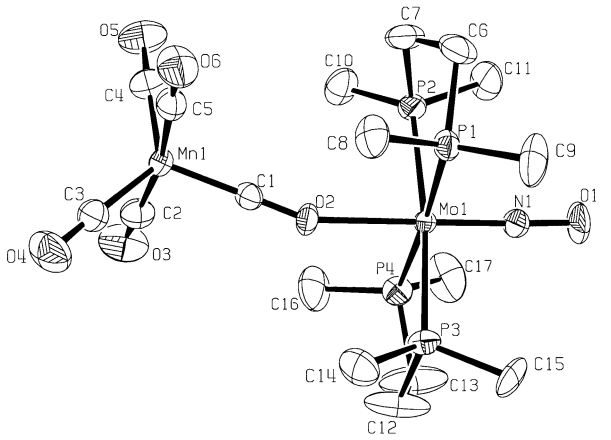

Figure 9. ORTEP plot of the structure of **12**. Displacement ellipsoids are drawn with 50% probability. The hydrogen atoms have been omitted for clarity.

Table 6. Selected Bond Lengths [Å] and Bond Angles [deg] of 12

Mo(1)−N(1)	1.761(3)	N(1)−Mo(1)−P(1)	89.93(12)
Mo(1)−O(2)	2.259(3)	N(1)−Mo(1)−P(2)	92.73(12)
Mo(1)−P(1)	2.4506(11)	N(1)−Mo(1)−P(3)	93.54(12)
Mo(1)−P(2)	2.4545(10)	N(1)−Mo(1)−P(4)	93.83(12)
Mo(1)−P(3)	2.4554(10)	P(1)−Mo(1)−P(2)	80.28(4)
Mo(1)−P(4)	2.4595(11)	P(3)−Mo(1)−P(4)	80.73(4)
N(1)−O(1)	1.220(4)	N(1)−Mo(1)−O(2)	178.09(14)
Mn(1)−C(1)	1.759(4)	C(1)−O(2)−Mo(1)	159.0(3)
Mn(1)−C(2)	1.831(5)	O(2)−C(1)−Mn(1)	179.2(3)
Mn(1)−C(3)	1.823(4)	C(1)−Mn(1)−C(2)	92.8(2)
Mn(1)−C(4)	1.826(5)	C(1)−Mn(1)−C(3)	115.06(15)
Mn(1)−C(5)	1.830(4)	C(1)−Mn(1)−C(4)	115.8(2)
C(1)−O(2)	1.180(5)	C(1)−Mn(1)−C(5)	95.60(19)
C(2)−O(3)	1.141(6)	C(3)−Mn(1)−C(2)	88.6(2)
C(3)−O(4)	1.154(5)	C(4)−Mn(1)−C(2)	88.3(2)
C(4)−O(5)	1.143(6)	C(3)−Mn(1)−C(5)	86.64(15)
C(5)−O(6)	1.143(5)	C(4)−Mn(1)−C(5)	89.3(2)

in the range 233.9−234.2 ppm are found, confirming the presence of metal-bound carbonyl groups. The IR spectrum of **12** (Nujol mull) shows among others a band at 1580 cm^{-1} corresponding to a ν(NO) vibration, and five bands at 2022, 1923, 1908, 1885, and 1746 cm^{-1} are assigned to ν(CO) vibrations. This five-band pattern of the IR spectrum is similar to that of $NaMn(CO)_5$,[20] revealing the presence of a $Mn(CO)_5$ fragment. A band at relatively low wavenumbers (1746 cm^{-1}) provides evidence for the bridging carbonyl ligand.[21] However, it should be mentioned that by IR spectroscopy alone the carbonyl coordination mode cannot unambiguously be distinguished from alternative binding ways.[21]

To elucidate the structure of complex **12**, especially with respect to the coordination mode of the bridging carbonyl group, a single-crystal X-ray diffraction study was carried out. Single crystals suitable for the diffraction analysis were obtained from diffusion of pentane into a toluene solution of **12**. An ORTEP drawing of **12** is shown in Figure 9. Selected bond distances and angles are listed in Table 6. The geometry of the $Mo(dmpe)_2(NO)$ fragment in **12** is very similar to those of all of the aforementioned structurally characterized complexes. The novel aspect of the structure of **12** is indeed the coordination mode of the bridging carbonyl group. It binds to manganese via carbon and to molybdenum via oxygen, acting as a μ-OC group. This binding feature remains a rarity[22,23] among the versatile bonding modes of CO groups. The reported complexes, which bear a μ-OC carbonyl, usually possess oxophilic main group metals, f group elements, or early transition metals as the acceptors of the O_{CO} atom. To our knowledge complex **12** is the first structurally characterized case with the oxygen of the μ-OC moiety binding to a mid transition metal center. The alternative metal−metal bonded structure $[(dmpe)_2(NO)Mo-Mn(CO)_5]$ isomeric to **12** is presumably not formed, because of a too weak heterobimetallic Mo−Mn interaction. The $Mn(CO)_5$ fragment in **12** adopts a trigonal-bipyramidal structure similar to those found in related complexes.[24] It is one of the equatorial carbonyl groups that acts as the bridging ligand connecting to the $Mo(dmpe)_2(NO)$ fragment. The angles of O(2)−C(1)−Mn(1) and C(1)−O(2)−Mo(1) are 179.2(3)° and 159.0(3)°, respectively. The latter shows a relatively large bend, which however resembles those found in previously reported examples of μ-OC bridges.[22,23] The average length of the terminal Mn−C bonds is 1.828(5) Å larger than the length of the bridging Mn−C bond of 1.759(4) Å, whereas the average distance of 1.145(5) Å for the terminal CO groups is shorter than the distance of 1.180(5) Å for the bridging C−O bond. The shortening of the Mn−C bond and the lengthening of the C−O bond for the μ-OC carbonyl group are consistent with the idea that the formation of the bridging bonds increases the participation of CO π^* character.[23]

The possibility of a double insertion of **3** into $Mn_2(CO)_{10}$, as it was the case for $Re_2(CO)_{10}$, has also been explored. Reaction of $Mn_2(CO)_{10}$ with up to 3 equiv of **3** was carried out in C_7D_8 at room temperature and monitored by NMR spectroscopy. Trace resonances for a double insertion product could presumably be identified in the reaction mixture, but the amount of the product was so small that any attempt of isolation failed.

Conclusions

The molybdenum hydride $Mo(dmpe)_2(H)(NO)$ (**3**) possesses due to its specific ligand sphere of a tetraphosphorus donor substitution pattern and the presence of the trans influence ligand nitrosyl a strong hydridic character of the Mo−H bond. This hydride is even more hydridic than *mer*-$Mo(CO)(H)(NO)(PMe_3)_3$. This was quantitatively demonstrated with DQCC and bond ionicity determinations of the corresponding deuterides obtained from T_{1min} measurements in solution and in solid state from the Pake doublets of static ^2H NMR spectra. In agreement with its enhanced hydridic properties, **3** exhibits a high propensity to undergo hydride transfer reactions, as demonstrated by its reactions with simple ketones and metal carbonyls, which by insertions led to alkoxy or formyl compounds. **3** was capable of reacting even twice with the Re−CO bonds of $Re_2(CO)_{10}$. The high activity of **3** may be attributed to the effect of its increased number of strongly σ-donating phosphorus ligands. This work therefore demonstrates the possibility of a tuning of the ionic or covalent character of L_nM-H bonds of metal hydrides via appropriate adjustment of the ancillary ligand spheres.

Experimental Section

All reactions and manipulations with air-sensitive compounds were performed under an atmosphere of dry nitrogen

using conventional Schlenk techniques or a glovebox. Solvents were dried by standard methods and freshly distilled under nitrogen before use. dmpe[26] and *trans*-$Mo(CO)_4(NO)(ClAlCl_3)$[27] were prepared following literature procedures. Other reagents were purchased from Fluka or Aldrich. NMR spectra were recorded on the following NMR spectrometers: Varian Gemini-300 instrument, ^1H at 300.1 MHz, ^{13}C at 75.4 MHz, ^{31}P at 121.5 MHz, ^{11}B at 96.2 MHz; Bruker DRX-500 instrument, ^1H at 500.2 MHz, ^{13}C at 125.8 MHz, ^{31}P at 202.5 MHz, ^{11}B at 160.5 MHz. $\delta(^1H)$ and $\delta(^{13}C)$ relative to $SiMe_4$, $\delta(^{31}P)$ relative to 85% H_3PO_4, $\delta(^{11}B)$ relative to $BF_3{\cdot}OEt_2$. IR spectra: Biorad FTS-45 instrument. Mass spectra: Finnigan-MAT-8400 spectrometer; FAB spectra in 3-nitrobenzyl alcohol matrix. Elemental analyses: Leco CHN(S)-932 instrument.

***trans*-Mo(Cl)(dmpe)$_2$(NO) (1).** A 40 mL autoclave was charged under nitrogen with a mixture of 0.84 g (2.06 mmol) of *trans*-$Mo(CO)_4(NO)(ClAlCl_3)$ and 1.0 g (6.66 mmol) of dmpe in 25 mL of THF and then heated to 160 °C. During this time the produced CO was released periodically from the autoclave under N_2 to facilitate the reaction. After 8 days the mixture was cooled to room temperature and then filtered. The filtrate was dried in vacuo, and the remaining residue was extracted with Et_2O. Concentration and chilling of the combined solutions to −30 °C afforded yellow crystals of **1**. Yield: 0.80 g (84%). IR (cm^{-1}, THF): 1553 (NO). ^1H NMR (C_6D_6): 1.35 (s, br, 24H, PMe), 1.45 (m, 4H, PCH_2), 1.24 (m, 4H, PCH_2'). $^{13}C\{^1H\}$ NMR (C_6D_6): 29.9 (quint, $^1J_{CP}$ = 10 Hz, PCH_2), 14.9 (quint, $^1J_{CP}$ = 5.3 Hz, PMe), 14.8 (quint, $^1J_{CP}$ = 5.3 Hz, PMe′). $^{31}P\{^1H\}$ NMR (C_6D_6): 35.4 (s). EI-MS: 462 (48, M^+), 431 (22, [M^+ − NO]), 371 (24, [M^+ − NO − $4Me_3$]), 312 (44, [M^+ − dmpe]), 282 (16, [M^+ − dmpe − NO]). Anal. Calcd for $C_{12}H_{32}ClMoNOP_4$: C 31.21, H 7.00, N 3.03. Found: C 31.54, H 6.93, N 3.00.

***trans*-Mo(η^1-BH_4)(dmpe)$_2$(NO) (2).** A 0.16 g (0.35 mmol) sample of **1** was dissolved in 20 mL of Et_2O, and then 0.04 g (1.84 mmol) of $LiBH_4$ was added. The resulting mixture was stirred at room temperature for 4 days, then the solvent was removed in vacuo. The residue was extracted with toluene until the solution remained colorless. The remaining solid was redissolved in Et_2O and cooled to −30 °C. After one night the Et_2O was removed again in vacuo and the residue extracted with toluene. This procedure was repeated four times. Combination of the extracts and removal of the toluene gave a yellow solid. Recrystallization from Et_2O at −30 °C afforded analytically pure crystals of **2**. Yield: 0.12 g (80%). IR (cm^{-1}, THF): 1567 (NO). ^1H NMR (C_6D_6): 1.40 (s, 12H, PMe), 1.26 (s, 12H, PMe′), 1.47 (m, 4H, PCH_2), 1.19 (m, 4H, PCH_2'), −2.26 (quart, br, $^1J_{HB}$ = 81 Hz, 4H, BH_4). $^{13}C\{^1H\}$ NMR (C_6D_6): 30.0 (quint, $^1J_{CP}$ = 10 Hz, PCH_2), 16.5 (quint, $^1J_{CP}$ = 6.0 Hz, PMe), 15.1 (quint, $^1J_{CP}$ = 5.4 Hz, PMe′). ^{11}B NMR (C_6D_6): −42.1 (quint, $^1J_{BH}$ = 81 Hz). $^{31}P\{^1H\}$ NMR (C_6D_6): 36.2 (s). EI-MS: 441 (11, M^+), 427 (86, [M^+ − BH_3]), 411 (21, [M^+ − NO]), Anal. Calcd for $C_{12}H_{36}BMoNOP_4$: C 32.67, H 8.24, N 3.18. Found: C 32.88, H 8.21, N 3.19.

***trans*-Mo(η^1-BD_4)(dmpe)$_2$(NO) (2a). 2a** was prepared in a procedure analogous to that for **2** except that $NaBD_4$ and LiCl were used as a substitute for $LiBD_4$ in the conversion of chloride **1**. $^{31}P\{^1H\}$ NMR (C_6D_6): 36.3 (t, $^2J_{PD}$ = 5 Hz). ^2H NMR (C_6H_6): −2.30 (m, br, DBD_3).

***trans*-Mo(dmpe)$_2$(H)(NO) (3).** A 0.18 g (0.41 mmol) sample of **2** and 0.36 g (3.24 mmol) of quinuclidine were dissolved in 15 mL of toluene. The resulting solution was stirred at room temperature for 48 h, then the solvent was removed in vacuo. The remaining residue was extracted with pentane. Removal of pentane at room temperature and subsequent sublimation of excess quinuclidine at 60 °C for 24 h in vacuo afforded the product of **3** as a yellow solid. Yield: 0.16 g (92%). IR (cm^{-1}, THF): 1557 (NO). ^1H NMR (C_6D_6): 1.47 (s, 12H, PMe), 1.27 (s, 12H, PMe′), 1.37 (m, 8H, PCH_2), −4.58 (quint, br, $^2J_{HP}$ = 29 Hz, 1H, MoH). $^{13}C\{^1H\}$ NMR (C_6D_6): 32.1 (quint, $^1J_{CP}$ = 11 Hz, PCH_2), 22.9 (quint, $^1J_{CP}$ = 6.6 Hz, PMe), 18.0 (quint, $^1J_{CP}$ = 4.4 Hz, PMe′). $^{31}P\{^1H\}$ NMR (C_6D_6): 44.2 (s). EI-MS: 427 (86, M^+), 412 (16, [M^+ − CH_3]), 397 (13, [M^+ − NO]), 337 (15, [M^+ − NO − 4Me]), 277 (11, [M^+ − dmpe]). Anal. Calcd for $C_{12}H_{33}MoNOP_4$: C 33.73, H 7.80, N 3.28. Found: C 34.10, H 7.66, N 3.00.

***trans*-Mo(dmpe)$_2$(D)(NO) (3a). 3a** was prepared from **2a** in a procedure analogous to that for **3**. $^{31}P\{^1H\}$ NMR (C_7D_8): 44.3 (t, $^2J_{PD}$ = 5 Hz). ^2H NMR (C_7H_8): −4.72 (m, MoD). IR (cm^{-1}, THF): 1542 (NO).

***mer*-Mo(CO)(D)(NO)(PMe_3)$_3$ (4).** At first the borodeuteride *mer*-Mo(η^1-BD_4)(CO)(NO)(PMe_3)$_3$ was prepared in a procedure analogous to that for *mer*-Mo(η^1-BH_4)(CO)(NO)-(PMe_3)$_3$ except that $NaBD_4$ and LiCl were used as a substitute for $LiBD_4$.[8] Then **4** was prepared from the borodeuteride in a procedure analogous to that for *mer*-Mo(CO)(H)(NO)(PMe_3)$_3$.[8] $^{31}P\{^1H\}$ NMR (C_7D_8): −3.80 (dt, $^2J_{PP}$ = 29 Hz, $^2J_{PD}$ = 5 Hz, 2 PMe_3 trans), −11.4 (tt, $^2J_{PP}$ = 29 Hz, $^2J_{PD}$ = 4 Hz, PMe_3 trans CO). ^2H NMR (C_7H_8): −1.90 (m, br, MoD). IR (cm^{-1}, hexane): 1916 (CO), 1597 (NO).

***trans*-Mo(dmpe)$_2$(NO)($OCHPh_2$) (5).** A mixture of 0.0210 g (0.049 mmol) of **3** and 0.0095 g (0.052 mmol) of benzophenone was dissolved in ca. 0.7 mL of C_7D_8. The reaction was monitored by ^1H NMR. After 2 h the reaction was complete. The solvent was removed in vacuo, and the remaining residue was extracted with pentane. The combined solutions were concentrated and cooled to −30 °C to give yellow crystals of **5**. Yield: 0.265 g (89%). IR (cm^{-1}, THF): 1528 (NO). ^1H NMR (C_6D_6): 7.32 (m, 4H, Ph), 7.10 (m, 4H, Ph), 6.95 (m, 2H, Ph), 5.03 (s, 1H, OCH), 1.34 (s, 12H, PMe), 1.19 (s, 12H, PMe′), 1.26 (m, 8H, PCH_2). $^{13}C\{^1H\}$ NMR (C_6D_6): 153.9, 127.7, 126.4, 125.5 (4s, Ph), 85.3 (quint, $^3J_{CP}$ = 3.9 Hz, OCH), 30.2 (quint, $^1J_{CP}$ = 9.5 Hz, PCH_2), 16.4 (quint, $^1J_{CP}$ = 4.2 Hz, PMe), 15.3 (quint, $^1J_{CP}$ = 5.3 Hz, PMe′). $^{31}P\{^1H\}$ NMR (C_6D_6): 31.9 (s). EI-MS: 610 (65, M^+), 459 (100, [M^+ − dmpe]), 426 (14, [M^+ − Ph_2CHO]), 396 (13, [M^+ − Ph_2CHO − NO]). Anal. Calcd for $C_{25}H_{43}MoNO_2P_4$: C 49.26, H 7.13, N 2.30. Found: C 49.24, H 7.22, N 2.31.

***trans*-Mo(dmpe)$_2$(NO)[OCH(CH_3)(Ph)] (6).** To a solution of 0.023 g (0.054 mmol) of **3** in ca. 0.7 mL of C_7D_8 in an NMR tube was added 6.5 μL (0.056 mmol) of acetophenone. The reaction was monitored at room temperature by ^1H NMR. After 1.5 h the reaction was complete. Then the solvent was removed in vacuo and the remaining residue recrystallized from pentane at −30 °C to afford **6** as a yellow solid. Yield: 0.025 g (85%). IR (cm^{-1}, THF): 1524 (NO). ^1H NMR (C_6D_6): 7.26−7.15 (m, 4H, Ph), 7.10−7.05 (m, 1H, Ph), 4.14 (quart, $^3J_{HH}$ = 6 Hz, 1H, OCH), 1.37 (m, 12H, PMe), 1.30 (m, 6H, PMe′), 1.22 (m, 6H, PMe′), 1.34 (m, 8H, PCH_2), 1.04 (d, $^3J_{HH}$ = 6 Hz, 3H, $-CH_3$). $^{13}C\{^1H\}$ NMR (C_6D_6): 155.2, 127.5, 125.9, 125.4 (4s, Ph), 77.5 (quint, $^3J_{CP}$ = 3.5 Hz, OCH), 31.8 (s, br, PCH_2), 16.0 (m, PMe), 15.7 (m, PMe′), 15.3 (m, PMe). $^{31}P\{^1H\}$ NMR (C_6D_6): 32.4 (m). EI-MS: 547 (88, M^+), 427 (32, [M^+ − MePhCHO]), 397 (100, [M^+ − dmpe]). Anal. Calcd for $C_{20}H_{41}MoNO_2P_4$: C 43.88, H 7.56, N 2.56. Found: C 44.07, H 7.36, N 2.62.

***trans*-Mo(dmpe)$_2$(NO)[OCH(CH_3)$_2$] (7).** A 4.4 μL (0.06 mmol) sample of acetone was added to a solution of 0.025 g (0.059 mmol) of **3** in ca. 0.7 mL of C_7D_8 in an NMR tube. The mixture was monitored by ^1H NMR. After 3 h the reaction was complete. The solvent was removed in vacuo and the residue was extracted with pentane. Concentration and chilling to −30 °C of the extracts produced a yellow solid of **7**. Yield: 0.023 g (80%). IR (cm^{-1}, THF): 1520 (NO). ^1H NMR (C_6D_6): 3.25 (hept, $^3J_{HH}$ = 6 Hz, 1H, OCH), 1.40 (s, br, 12H, PMe), 1.29 (s, br, 12H, PMe′), 1.35 (m, 8H, PCH_2), 0.87 (d, $^3J_{HH}$ = 6 Hz, 6H, $-CH_3$). $^{13}C\{^1H\}$ NMR (C_6D_6): 69.3 (quint, $^3J_{CP}$ = 3.6 Hz, OCH),

(26) Burt, R. J.; Chatt, J.; Hussain, W.; Leigh, G. J. *J. Organomet. Chem.* **1979**, *182*, 203.
(27) Seyferth, K.; Taube, R. *J. Organomet. Chem.* **1982**, *229*, 275; Cheng, T. Y.; Southern T. S.; Hillhouse, G. L. *Organometallics* **1997**, *16*, 2335.

Table 7. Crystallographic Data and Structure Refinement Parameters for 1, 2, and 8

	1	2	8
formula	$C_{12}H_{32}ClMoNOP_4$	$C_{12}H_{36}BMoNOP_4$	$C_{17}H_{33}FeMoNO_6P_4$
color	yellow	yellow	orange
cryst dimens (mm)	0.40 × 0.33 × 0.30	0.49 × 0.42 × 0.30	0.44 × 0.21 × 0.20
temp (K)	173(2)	173(2)	183(2)
cryst syst	monoclinic	monoclinic	orthorhombic
space group (No.)	$P2_1/n$ (14)	$P2_1/n$ (14)	$Cmc2_1$ (36)
a (Å)	9.5217(8)	8.4970(7)	14.9570(10)
b (Å)	11.3764(7)	13.2450(10)	15.3181(11)
c (Å)	10.0280(8)	9.7498(8)	12.0282(9)
α (deg)	90	90	90
β (deg)	92.438(10)	94.501(10)	90
γ (deg)	90	90	90
V (Å^3)	1085.28(14)	1093.89(15)	2755.8(3)
Z	2	2	4
fw	461.66	441.05	623.11
d(calcd) (g cm^{-3})	1.413	1.339	1.502
abs coeff (mm^{-1})	1.019	0.888	1.243
F(000)	476	460	1272
2θ scan range (deg)	6.80 < 2θ < 60.48	6.86 < 2θ < 60.72	7.62 < 2θ < 60.58
no. of unique data	3081	3026	3918
no. of data obsd [$I > 2\sigma(I)$]	2623	2582	3531
abs corr	numerical	numerical	numerical
solution method	Patterson	Patterson	Patterson
no. of params refined	110	108	155
R, wR2 (%) all data	2.69, 5.78	5.12, 12.79	4.48, 11.66
R1, wR2 (obsd) (%)[a]	2.18, 5.53	4.26, 12.25	3.51, 9.17
goodness-of-fit	1.03	1.21	1.125

[a] $R1 = \sum(F_o - F_c)/\sum F_o$; $I > 2\sigma(I)$; $wR2 = \{\sum w(F_o^2 - F_c^2)^2/\sum w(F_o^2)^2\}^{1/2}$.

30.4 (quint, $^1J_{CP}$ = 9.8 Hz, PCH_2), 29.9 (s, CH_3), 15.4 (m, PMe). $^{31}P\{^1H\}$ NMR (C_6D_6): 32.8 (s). EI-MS: 485 (70, M^+), 426 (28, [M^+ − Me_2CHO]), 396 (28, [M^+ − Me_2CHO − NO]), 335 (100, [M^+ − dmpe]). Anal. Calcd for $C_{15}H_{39}MoNO_2P_4$: C 37.12, H 8.12, N 2.89. Found: C 37.23, H 8.44, N 2.96.

***trans*-Mo(dmpe)$_2$(NO)[(μ-OCH)Fe(CO)$_4$] (8).** A 0.028 g (0.066 mmol) sample of **3** was dissolved in ca. 0.7 mL of C_7D_8 in an NMR tube, and 9.0 μL (0.068 mmol) of iron pentacarbonyl was added. In a few minutes some crystals precipitated from the solution and the reaction was complete (^{1}H NMR monitoring). The solvent was removed in vacuo, and the remaining residue was dissolved in ca. 0.5 mL of THF. Diffusion of pentane into the THF solution afforded **8** as orange crystals. Yield: 0.033 g (81%). IR (cm^{-1}, THF): 2032, 1949, 1918 ($Fe(CO)_4$), 1570 (NO). ^{1}H NMR (C_6D_6): 13.52 (m, 1H, OCH), 1.23 (m, 8H, PCH_2), 1.14 (s, br, 12H, PMe), 1.11 (s, br, 12H, PMe′). $^{13}C\{^1H\}$ NMR (C_6D_6): 299.3 (quint, $^3J_{CP}$ = 4 Hz, −OCH−), 218.5 (s, $Fe(CO)_4$), 29.2 (quint, $^1J_{CP}$ = 10 Hz, PCH_2), 14.3 (m, PMe). $^{31}P\{^1H\}$ NMR (C_6D_6): 35.3 (s). EI-MS: 473 (40, [M^+ − dmpe]), 426 (83, [M^+ − $Fe(CO)_4CHO$]), 411 (31, [M^+ − $Fe(CO)_4CHO$ − CH_3]), 396 (18, [M^+ − $Fe(CO)_4CHO$ − NO]). Anal. Calcd for $C_{17}H_{33}FeMoNO_6P_4$: C 32.76, H 5.35, N 2.25. Found: C 33.06, H 5.52, N 2.27.

***trans*-Mo(dmpe)$_2$(NO)[(μ-OCH)Re$_2$(CO)$_9$] (9).** To a solution of 0.023 g (0.054 mmol) of **3** in ca. 0.7 mL of C_7D_8 was added 0.035 g (0.054 mmol) of dirhenium decacarbonyl. In a few minutes the $Re_2(CO)_{10}$ dissolved and the reaction was complete (NMR monitoring). The solvent was removed in vacuo, and the remaining residue was extracted with Et_2O. Concentration and cooling to −30 °C of the extracts gave orange crystals of **9**. Yield: 0.050 g (86%). IR (cm^{-1}, THF): 2094, 2031, 2009, 1981, 1952, 1939, 1911 ($Re_2(CO)_9$), 1571 (NO). ^{1}H NMR (C_7D_8): 14.57 (s, 1H, OCH), 1.27 (m, 8H, PCH_2), 1.10 (s, br, 24H, PMe). $^{13}C\{^1H\}$ NMR (C_7D_8): 298.4 (m, OCH), 200.9, 196.2, 192.2 (3s, $Re_2(CO)_9$), 29.6 (quint, $^1J_{CP}$ = 10 Hz, PCH_2), 14.6 (quint, $^1J_{CP}$ = 5.4 Hz, PMe), 14.4 (quint, $^1J_{CP}$ = 5.4 Hz, PMe′). $^{31}P\{^1H\}$ NMR (C_7D_8): 36.0 (s). EI-MS: 749 (28, [M^+ − 2dmpe − NO]), 662 (50, [M^+ − H − $Re(CO)_5$ − NO − $4CH_3$]), 632 (32, [M^+ − H − $Re(CO)_5$ − NO − $6CH_3$]), 602 (18, [M^+ − H − $Re(CO)_5$ − dmpe]), 422 (46, [M^+ − H − $Re(CO)_5$ − 2dmpe − NO]). Anal. Calcd for $C_{22}H_{33}MoNO_{11}P_4Re_2$: C 24.47, H 3.09, N 1.30. Found: C 24.77, H 3.08, N 1.18.

(ON)(dmpe)$_2$Mo(μ-OCH)Re$_2$(CO)$_8$(μ-CHO)Mo(dmpe)$_2$-(NO) (10). **3** (0.0375 g, 0.088 mmol) and $Re_2(CO)_{10}$ (0.0143 g, 0.022 mmol) were treated in toluene (ca. 2 mL). In a few minutes the $Re_2(CO)_{10}$ dissolved completely and a yellow solution was obtained. Diffusion of pentane into this solution afforded yellow crystals. IR (cm^{-1}, THF): 2048, 1996, 1881 ($Re_2(CO)_8$), 1565(NO). ^{1}H NMR (C_7D_8): 14.66 (s, 2H, OCH), 1.27 (m, 16H, PCH_2), 1.14 (s,br, 48H, PMe). $^{13}C\{^1H\}$ NMR (C_7D_8): 298.9 (m, OCH), 207.1, 200.8 (2s, $Re_2(CO)_8$), 29.9 (quint, $^1J_{CP}$ = 10 Hz, PCH_2), 14.9 (quint, $^1J_{CP}$ = 5 Hz, PMe), 14.7 (quint, $^1J_{CP}$ = 5 Hz, PMe′). $^{31}P\{^1H\}$ NMR (C_7D_8): 36.5 (s). Anal. Calcd for $C_{34}H_{66}Mo_2N_2O_{12}P_8Re_2$: C 27.10, H 4.42, N 1.86. Found: C 32.05, H 4.68, N 1.75. An analytically pure sample could not be obtained. But crystals suitable for X-ray diffraction study were selected from the mixture.

***trans*-Mo(dmpe)$_2$(NO)[(μ-OC)Mn(CO)$_4$] (12).** A 0.018 g (0.042 mmol) sample of **3** was dissolved in ca. 0.7 mL of C_7D_8. To this solution was added 0.017 g (0.044 mmol) of dimanganese decacarbonyl. The reaction was monitored by ^{1}H NMR. After 2 days the solvent was removed and the residue was dissolved in toluene. Diffusion of pentane into the toluene solution afforded yellow crystals of **12**. Yield: 0.019 g (73%).

Alternative method: to a solution of 0.021 g (0.049 mmol) of **3** in ca. 0.7 mL of C_7D_8 was added 0.0096 g (0.049 mmol) of manganese pentacarbonyl hydride, which was prepared according to a literature procedure.[28] H_2 gas liberated immediately and in a few minutes the reaction was complete (NMR monitoring). The product was isolated by the procedure described above in a yield of 90% (0.028 g). IR (cm^{-1}, Nujol): 2022(w), 1923(m), 1908(m), 1885(s) ($Mn(CO)_4$), 1746(s) (Mn−CO−Mo), 1580(s) (NO). ^{1}H NMR (C_6D_6): 1.21 (m, 4H, PCH_2), 1.02 (m, 4H, PCH_2′), 1.16 (s, br, 12H, PMe), 1.07 (s, br, 12H, PMe′). $^{13}C\{^1H\}$ NMR (C_6D_6): 234.1 (m, MnCO), 29.1 (quint, $^1J_{CP}$ = 10 Hz, PCH_2), 14.3 (m, PMe). $^{31}P\{^1H\}$ NMR (C_6D_6): 36.0 (s). Anal. Calcd for $C_{17}H_{32}MnMoNO_6P_4$: C 32.86, H 5.20, N 2.26. Found: C 33.00, H 4.86, N 2.26.

X-ray Crystal Structure Analyses. The intensity diffraction data were collected at 173(2) K (**1**, **2**) and 183(2) K (**8**, **9**,

(28) Sanders, J. R. *J. Chem. Soc., Dalton Trans.* **1973**, 748; **1975**, 2340.

Table 8. Crystallographic Data and Structure Refinement Parameters for 9, 10, and 12

	9	**10**	**12**
formula	$C_{22}H_{33}MoNO_{11}P_4Re_2$	$C_{41}H_{74}Mo_2N_2O_{12}P_8Re_2$	$C_{17}H_{32}MnMoNO_6P_4$
color	orange	yellow	yellow
cryst dimens (mm)	0.34 × 0.33 × 0.20	0.26 × 0.24 × 0.16	0.33 × 0.26 × 0.14
temp (K)	183(2)	183(2)	183(2)
cryst syst	monoclinic	orthorhombic	triclinic
space group (No.)	$P2_1$ (4)	$Fdd2$ (43)	$P\bar{1}$ (2)
a (Å)	10.7609(9)	34.9624(16)	9.4800(8)
b (Å)	12.4912(11)	65.681(3)	9.7992(9)
c (Å)	12.8377(11)	10.5624(6)	16.3841(15)
α (deg)	90	90	105.481(10)
β (deg)	93.193(10)	90	95.446(11)
γ (deg)	90	90	109.324(10)
V (Å^3)	1722.9(3)	24255(2)	1355.8(2)
Z	2	16	2
fw	1079.71	1599.06	621.20
d(calcd) (g cm^{-3})	2.081	1.752	1.522
abs coeff (mm^{-1})	7.602	4.646	1.193
F(000)	1024	12544	632
2θ scan range (deg)	5.82 < 2θ < 60.84	4.08 < 2θ < 47.36	5.60 < 2θ < 60.54
no. of unique data	10 198	9113	7353
no. of data obsd [$I > 2\sigma(I)$]	8034	8635	5864
abs corr	numerical	numerical	numerical
solution method	Patterson	Patterson	Patterson
no. of params refined	334	622	279
R, wR2 (%) all data	7.72, 16.10	3.51, 8.26	5.45, 14.13
R1, wR2 (obsd) (%)[a]	6.00, 15.02	3.34, 8.20	3.98, 11.54
goodness-of-fit	1.063	1.106	1.149

[a] $R1 = \sum(F_o - F_c)/\sum F_o$; $I > 2\sigma(I)$; $wR2 = \{\sum w(F_o^2 - F_c^2)^2/\sum w(F_o^2)^2\}^{1/2}$.

10, **12**) using an imaging plate detector system (Stoe IPDS) with graphite-monochromated Mo Kα radiation. A total of 150, 129, 167, 120, 260, and 167 images were exposed at constant times of 1.50, 1.80, 2.50, 3.50, 3.00, and 3.00 min/image for compounds **1**, **2**, **8**, **9**, **10**, and **12**, respectively. The crystal-to-image distances were set to 50 mm, except for compound **10**, which had a necessary large distance of 82 mm. The corresponding θ_{max} values were 30.24°, 30.36°, 30.29°, 30.42°, 23.68°, and30.27°, respectively. ϕ-oscillation (**10**, **12**) or rotation scan modes (**1**, **2**, **8**, **9**) were selected for the ϕ increments of 1.2°,1.4°, 1.2°, 1.5°, 0.7°, and1.2° per exposure in each case. Total exposure times for the six compounds were 14, 13, 19, 15, 31, and 20 h in the order of the complexes given above. After integrations and corrections for Lorentz and polarization effects, a total of 8000 reflections were selected out of the whole limiting sphere for the cell parameter refinements. A total of 11 098, 11 328, 16 263, 14 313, 27 084, and 15 938 reflections were collected, of which 3081, 3026, 3918, 10198, 9113, and 7353 reflections were unique (R_{int} = 4.54%, 3.08%, 3.07%, 7.66%, 3.68%, and 2.98%); data reduction and numerical absorption correction used 14, 15, 15, 15, 13, and 9 indexed crystal faces.[29]

The structures were solved by the Patterson method using the Program SHELXS-97,[30] and they were refined with SHELXL-97.[31] The absolute structure was determined by using Flack's x-parameter refinement.[32] The absolute structure parameter x for **8**, **9**, and **10** was −0.01(3), 0.520(17), and 0.224(5), respectively. Merohedrical twinning was observed for **9** and **10** with an appoximate twin ratio of 1:1 and 1:4, respectively. The X-ray data collections and the processing parameters are given in Table 7 and Table 8.

Acknowledgment. Financial support from the Swiss National Science Foundation is gratefully acknowledged.

Supporting Information Available: Tables of crystal data and structure refinement parameters, atomic coordinates, bond lengths, bond angles, anisotropic displacement parameters, and hydrogen coordinates of **1**, **2**, **8**, **9**, **10**, and **12**. Additional IR and NMR spectra of **10**. This material is available free of charge via the Internet at http://pubs.acs.org.

OM021032T

(29) Stoe IPDS software for data collection, cell refinement and data reduction, Version 2.87-2.92 (the latter used for **5**); Stoe & Cie: Darmstadt, Germany, 1997−1999.

(30) SHELXS-97: Sheldrick, G. M. *Acta Crystallogr.* **1990**, *46A*, 467.

(31) SHELXL-97: Sheldrick, G. M. *Program for the Refinement of Crystal Structures*; University of Göttingen: Germany, 1997.

(32) (a) Flack, H. D. *Acta Crystallogr.* **1983**, *A39*, 876. (b) Flack, H. D.; Bernardinelli, G. *Acta Crystallogr.* **1999**, *A55*, 908.